Chiral Peptide Nucleic Acids (PNAs): Helix Handedness and DNA Recognition

Stefano Sforza,[a] Gerald Haaima,[b] Rosangela Marchelli,*[a] Peter E. Nielsen*[c]

Keywords: DNA recognition / Helical structures / Induced chirality / Peptide nucleic acid / Thermal stability

Peptide Nucleic Acids (PNAs) are DNA mimics in which the deoxyribose phosphate backbone has been replaced by a pseudo-peptide skeleton composed of *N*-(2-aminoethyl)-glycine units; they bind to complementary DNA strands with high affinity and selectivity. In order to study the effect of stereogenic centers within the backbone on PNA preorganization and DNA binding properties, chiral PNA decamers were synthesized which contained thymine monomers derived from L-Leu and D- or L-Lys inserted either at C-terminus and/or in the middle of an achiral PNA strand. PNAs containing three chiral thymine monomers derived from L-Leu, D- or L-Lys, L-Asp, or D-Glu were also synthesized. CD spectral analyses showed that a charged chiral monomer inserted in the middle of the strand is able to induce a strong preference in the helix handedness of a PNA-PNA duplex. The effect is increased by the presence of three chiral charged monomers. The L-Lys- and L-Asp-PNAs induced a preference for the left-handed and the D-Lys and D-Glu-PNAs for the right-handed conformation. As expected, the PNA-DNA duplexes are dominated by the DNA strand and thus are right-handed with both D- and L-PNAs. However, the D-PNAs, being inherently right-handed, lead to more stable PNA-DNA duplexes than the L-PNAs. The lysine-based PNAs form more stable complexes with the DNA at low ionic strength, due to the electrostatic interactions between the charged lysine side chain and DNA.

Introduction

Peptide nucleic acids (PNAs) are DNA mimics in which the deoxyribose phosphate backbone has been replaced by a polyamide skeleton composed of *N*-(2-aminoethyl)glycine units, with the nucleobases linked to the glycine nitrogen via a methylene carbonyl group.[1−2] PNAs bind efficiently and with high sequence selectivity to both single stranded RNA, DNA, and PNA as well as to double stranded DNA.[3]

In particular, PNA oligomers bind to complementary DNA oligonucleotides forming helical PNA-DNA duplexes that are in general more stable than the corresponding DNA-DNA duplexes.[4] Furthermore, PNA oligomers of complementary sequences have been shown to hybridize forming helical PNA-PNA duplexes of higher thermal stabilities (T_m) than those observed for the PNA-RNA and the PNA-DNA duplexes.[5] The results obtained so far show that PNA has many of the properties required for an antisense or antigene drug including high biological and chemical stability.[6]

However, recent structural studies by NMR and X-ray crystallography on PNA complexes (PNA-RNA,[7] PNA-DNA,[8] and especially a PNA-PNA duplex[9] and a PNA_2-DNA triplex[10]), have indicated that the conformation inherently adopted by PNA is not optimal for hybridization to complementary RNA or DNA. PNA seems to prefer a wider helix (28 Å) with a much larger pitch (18 bp) than DNA or RNA.[9]

Since the first reports on PNA, several strategies of structure modification have been explored in order to better understand the chemical and structural features which determine PNA-DNA molecular recognition. The basic structure and the constrained flexibility of the PNA backbone appear to be of fundamental importance.[6]

PNAs are inherently achiral, and therefore PNA-PNA duplexes are racemic mixtures of double helices of opposite handedness.[5] A preferred handedness in the duplex may be induced by linking a chiral amino acid (e.g. L- or D-lysine) to the C-terminus of the strand. The process was described as "a seeding of chirality, beginning from the terminal base pair and migrating through the stack of the bases". As expected, helices induced by D- and L-lysine were found to be of opposite helicity.[11] By substituting L-lysine with L-phenylalanine or L-isoleucine the preferred helical form was maintained, whereas with L-glutamic acid the opposite handedness was preferred. These results indicate that the preferred helical sense of a PNA-PNA duplex is not related in a simple way to the absolute configuration of the amino acid attached to the carboxy-terminus.

More recently, with chiral monomers based on different amino acids inserted into the backbone of the PNA strand, it was found that the type of amino acid side chain and the configuration of the chiral center affect the stability of PNA-DNA duplexes.[12]

[a] Dipartimento di Chimica Organica ed Industriale, Università di Parma,
Viale delle Scienze, I-43100 Parma, Italy
Fax: (internat.) +39−0521905472
E-mail: marchell@ipruniv.cce.unipr.it
[b] Department of Organic Chemistry, The H. C. Ørsted Institute, Universitetsparken 5, DK-2100 Copenhagen, Denmark
[c] Center for Biomolecular Recognition, Panum Institute, Department of Biochemistry,
Blegdamsvej 3c, DK-2200 Copenhagen, Denmark
Fax: (internat.) +45−31396042
E-mail: pen@imbg.ku.dk

  1434−193X/99/0101−0197 $ 17.50+.50/0

These monomers allow the investigation of having specifically positioned stereogenic centers within the PNA oligomer. Thus, it is of a general interest to investigate how many stereogenic centers inserted at which positions of a PNA oligomer can induce a preferred handedness of the single or double stranded PNA, and if an eventual stereochemical preorganization of PNAs can favor the DNA recognition process.

In order to establish the influence of chirality on the induction of helical structures and to correlate the handedness of the PNA-PNA helix with the DNA affinity, PNA-PNA and PNA-DNA hybrids were studied by means of thermal denaturation measurements (T_m, from which the thermodynamic parameters were derived) and CD spectroscopy. The handedness of PNA helices is discussed on the base of circular dicroism spectra.

Chiral PNA monomers derived from polar (D- and L-Lys, D-Asp, and L-Glu) and apolar (L-Leu) amino acids (Figure 1) were inserted centrally and/or distally in a PNA 10-mer by means of a standard procedure on a solid phase:[15] H-GTAGA*T*CACT-NH_2, H-GTAGATCAC*T*-NH_2, H-G*T*AGA*T*CAC*T*-NH_2 (the chiral monomer is represented as *T*).

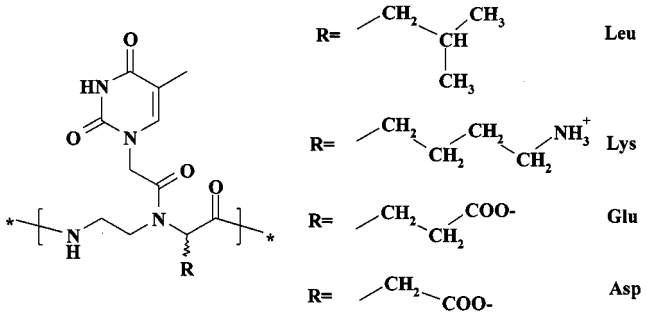

(**1**) - $T_{L\text{-Leu}}$ (C-ter.) H-GTAGATCAC$\mathbf{T_{L\text{-Leu}}}$-$NH_2$

(**2**) - $T_{L\text{-Leu}}$ (middle) H-GTAGA$\mathbf{T_{L\text{-Leu}}}$CACT-$NH_2$

(**3**) - $3T_{L\text{-Leu}}$ H-G$\mathbf{T_{L\text{-Leu}}}AGA\mathbf{T_{L\text{-Leu}}}CAC\mathbf{T_{L\text{-Leu}}}$-$NH_2$

(**4**) - $T_{L\text{-Lys}}$ (C-ter.) H-GTAGATCAC$\mathbf{T_{L\text{-Lys}}}$-$NH_2$

(**5**) - $T_{D\text{-Lys}}$ (C-ter.) H-GTAGATCAC$\mathbf{T_{D\text{-Lys}}}$-$NH_2$

(**6**) - $T_{L\text{-Lys}}$ (middle) H-GTAGA$\mathbf{T_{L\text{-Lys}}}$CACT-$NH_2$

(**7**) - $T_{D\text{-Lys}}$ (middle) H-GTAGA$\mathbf{T_{D\text{-Lys}}}$CACT-$NH_2$

(**8**)- $3T_{L\text{-Lys}}$ H-G$\mathbf{T_{L\text{-Lys}}}AGA\mathbf{T_{L\text{-Lys}}}CAC\mathbf{T_{L\text{-Lys}}}$-$NH_2$

(**9**) - $3T_{D\text{-Lys}}$ H-G$\mathbf{T_{D\text{-Lys}}}AGA\mathbf{T_{D\text{-Lys}}}CAC\mathbf{T_{D\text{-Lys}}}$-$NH_2$

(**10**) -$3T_{L\text{-Asp}}$ H-G$\mathbf{T_{L\text{-Asp}}}AGA\mathbf{T_{L\text{-Asp}}}CAC\mathbf{T_{L\text{-Asp}}}$-$NH_2$

(**11**) - $3T_{D\text{-Glu}}$ H-G$\mathbf{T_{D\text{-Glu}}}AGA\mathbf{T_{D\text{-Glu}}}CAC\mathbf{T_{D\text{-Glu}}}$-$NH_2$

Figure 1. Structures of the monomers containing chiral amino acids and thymine as the base and the PNAs synthesized

Results and Discussion

PNA Synthesis

The T_{Leu}, T_{Lys}, T_{Glu}, T_{Asp} monomers were prepared as described in literature.[12−13] PNAs incorporating $T_{L\text{-Leu}}$ (**2**, **3**), $T_{L\text{-Lys}}$ (**6**, **8**), $T_{L\text{-Asp}}$ (**10**), and $T_{D\text{-Glu}}$ (**11**) monomers were synthesized as previously described.[12,13,15]

The oligomerization of PNAs incorporating $T_{L\text{-Leu}}$ (**1**), $T_{L\text{-Lys}}$ (**4**), and $T_{D\text{-Lys}}$ (**5**, **7**, **9**) monomers was performed by means of the standard procedure on a (4-methylbenzhydryl)amine resin with HBTU/diethylcyclohexylamine in DMF/pyridine as coupling reagent. The free PNAs were cleaved from the resin using a TFMSA/TFA mixture, purified by HPLC and characterized by MALDI-TOF mass spectrometry.

The integrity of the stereogenic centers during the synthesis of the monomers and the oligomers was verified by chiral GC.[14]

Duplex Formation and Stability

PNAs containing L-Leu and D- and L-Lys were hybridized to the complementary achiral parallel or antiparallel PNA (H-CATCTAGTGA-NH_2 and H-AGTGATCTAC-NH_2) and to the complementary parallel or antiparallel DNA (5′-dCATCTAGTGA-3′ and 5′-dAGTGATCTAC-3′). Thermal stabilities (T_m) of the hybrids were determined by UV spectroscopy and compared with those obtained for the achiral 10-mer PNA of the same sequence (H-GTAGATCACT-NH_2) hybridized to the same targets. The results are summarized in Table 1.

As expected,[4−5] the chiral PNAs bound considerably better to the complementary PNA in the antiparallel rather than in the parallel orientation. The presence of three chiral monomers in the strands, both in the T_{Leu}- and in the T_{Lys}-PNAs, caused a decrease of stability for both the parallel and the antiparallel PNA-PNA duplexes, whereas one chiral lysine monomer inserted at the C-terminus exerted a positive effect.

The type of the amino acid side chain affected the PNA-DNA duplex stability in a different way. The T_{Leu}-PNAs showed decreased affinity for DNA, the effect being more pronounced for the PNAs containing three chiral monomers.

In contrast, several T_{Lys}-PNAs showed a higher affinity for DNA than the achiral PNA, probably due to the electrostatic interactions between the positively charged lysine and the DNA phosphate groups. Moreover, the antiparallel and the parallel PNA-DNA duplexes showed an opposite enantioselectivity. In particular, with T_{Lys}-PNAs bearing the chiral monomer in the middle or with three chiral monomers, the D-enantiomers (**7**) and (**9**) showed a relative preference for antiparallel complexation, whereas the L-enantiomers (**6**) and (**8**) bound relatively stronger in the parallel mode compared to the achiral PNA. In contrast, the PNAs incorporating T_{Lys} monomers at the C-terminus (**4**) and (**5**) did not show a significant enantioselectivity. The en-

Table 1. Melting temperatures (T_m, °C)[a] of L-leucine and D- and L-lysine-based PNAs and comparison to an achiral PNA[b] (ΔT_m, °C, in brackets)

PNA	PNA/PNA antiparallel	PNA/PNA parallel	Chirality	PNA/DNA antiparallel	PNA/DNA parallel
T_{Leu} (C-term.)	66 (+1)	44 (−4)	L (**1**)	46 (−3)	38 (−1)
T_{Leu} (middle)	63 (−2)	42 (−6)	L (**2**)	47 (−2)	39 (0)
$3T_{Leu}$	58 (−7)	38 (−10)	L (**3**)	45 (−4)	31 (−8)
T_{Lys} (C-term.)	68 (+3)	45 (−3)	L (**4**)	52 (+3)	38 (−1)
			D (**5**)	51 (+2)	39 (0)
T_{Lys} (middle)	65 (0)	44 (−4)	L (**6**)	47 (−2)	44 (+5)
			D (**7**)	51 (+2)	40 (+1)
$3T_{Lys}$	63 (−2)	41 (−7)	L (**8**)	49 (0)	42 (+3)
			D (**9**)	53 (+4)	38 (−1)

[a] Measurements were made in a 10 mM phosphate buffer, 100 mM NaCl, 0.1 mM EDTA, pH = 7.0. The melting temperatures for the PNA-PNA duplexes are the average of the results obtained with the two enantiomers. Estimated deviations: ±1°C. – [b] PNA sequence: H-GTAGATCACT-NH_2.

anctioselectivity and the orientation selectivity of Lys-PNAs are schematically shown in Figures 2 and 3.

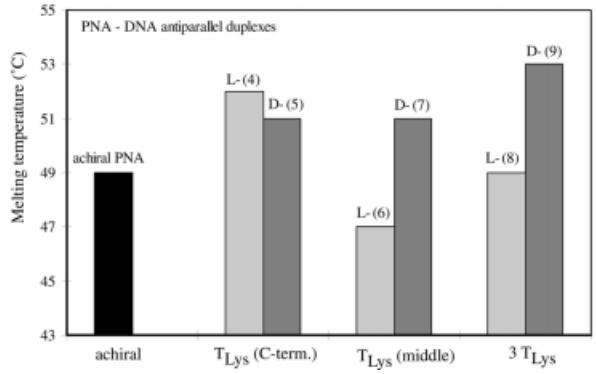

Figure 2. Melting temperatures of Lys-PNA-DNA antiparallel duplexes compared to the achiral PNA-DNA antiparallel duplex (estimated deviations ±1°C)

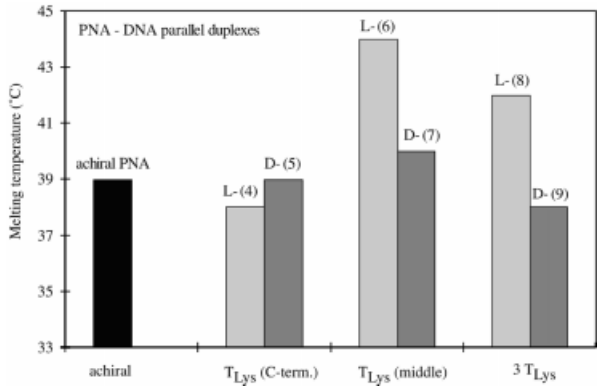

Figure 3. Melting temperatures of Lys-PNA-DNA parallel duplexes compared to the achiral PNA-DNA parallel duplex (estimated deviations ±1°C)

From these results, it is clear that for both PNA-PNA and PNA-DNA duplexes the stability depends on the number of chiral monomers inserted, on their position in the strand and on the nature of the amino acid side chain. In particular, with the Lys-PNAs, it has been demonstrated that the configuration of the stereogenic center can influence the binding orientation, thus exerting a certain degree of direction control.

Thermodynamic Parameters

Thermodynamic parameters for duplex formation can be extracted from experimental T_m measurements via determination of the concentration dependence of the T_m.[16] For the association of two non-self-complementary strands, the relationship between T_m and the total strand concentration Ct is given by the following equation:

$$1/T_m = (R/\Delta H°)\ln Ct + (\Delta S° - R\ln 4)/\Delta H°$$

By applying this equation, the thermodynamic parameters for the formation of the antiparallel duplexes were obtained (Tables 2 and 3). The measurements were made over a 100-fold concentration range in solutions with a low salt concentration (10 mM phosphate buffer, NaCl not present) in order to better evaluate the effects of the electrostatic interactions. So the results are not directly comparable with those reported in Table 1 (10 mM phosphate buffer, 100 mM NaCl).

The formation of PNA-PNA and PNA-DNA complexes, as also reported previously,[17] was accompanied to large enthalpy gains and entropy losses, in agreement with the formation of the more rigid duplex structures.

Table 2. Thermodynamic parameters[a] for antiparallel T_{Leu}-PNA-PNA and T_{Lys}-PNA-PNA duplex association

PNA in PNA/PNA duplex	$\Delta H°$ kJ/mol	$\Delta S°$ J/mol K	$\Delta G°_{298K}$ kJ/mol	$\Delta G°_{328K}$ kJ/mol
Achiral	−404	−1079	−82.4	−49.9
T_{Leu} (C-term.) (**1**)	−390	−1045	−78.3	−47.0
T_{Leu} (middle) (**2**)	−357	−960	−70.6	−41.8
T_{Lys}(middle) (**7**),(**8**)	−415	−1124	−79.7	−45.8
$3T_{Lys}$ (**11**),(**12**)	−431	−1182	−78.7	−43.2

[a] Errors in the given values were estimated as ±5%. Measurements were made in a 10 mM phosphate buffer, 0.1 mM EDTA, pH = 7.0.

Table 3. Thermodynamic parameters[a] for antiparallel T_{Leu}-PNA-DNA and T_{Lys}-PNA-DNA duplex association

PNA in PNA/DNA duplex	$\Delta H°$ kJ/mol	$\Delta S°$ J/mol K	$\Delta G°_{298K}$ kJ/mol	$\Delta G°_{328K}$ kJ/mol
Achiral	−286	−772	−56.0	−32.8
$T_{L\text{-}Leu}$ (C-ter.) (**1**)	−287	−776	−55.4	−32.1
$T_{L\text{-}Leu}$ (middle) (**2**)	−301	−830	−53.1	−28.2
$T_{L\text{-}Lys}$(middle) (**6**)	−370	−1036	−61.5	−29.7
$T_{D\text{-}Lys}$(middle) (**7**)	−325	−886	−61.3	−34.7
$3T_{L\text{-}Lys}$ (**8**)	−543	−1542	−83.5	−37.3
$3T_{D\text{-}Lys}$ (**9**)	−559	−1574	−90.2	−42.8
	−224[b]	−644[b]	−51.8[b]	−32.5[b]

[a] Errors in the given values were estimated as ±5%. Measurements were made in a 10 mM phosphate buffer, 0.1 mM EDTA, pH = 7.0. — [b] Measurements were made in a 10 mM phosphate buffer, 140 mM KCl, 0.1 mM EDTA, pH = 7.0.

The presence of chiral monomers in one PNA strand resulted in only minor changes in the overall enthalpic stabilization of the PNA-PNA duplexes (Table 2), as compared with the corresponding achiral PNA duplexes. In particular, the presence of a T_{Leu} monomer gives rise to a less favorable enthalpic variation, whereas the T_{Lys} monomers induce a more favorable enthalpic variation and a less favorable entropic change.

In contrast, for the PNA-DNA duplexes (Table 3), the presence of chiral monomers (either T_{Leu} or T_{Lys}) generally gave rise to more favorable enthalpy. The T_{Leu}-PNAs produced very small differences in DNA binding, if compared to achiral PNA, whereas T_{Lys}-PNAs gave rise to higher enthalpy gains, the effect being dependent on the number of lysine residues and, to a lesser extent, on their absolute configuration. It is worth noticing that $3T_{Lys}$-PNAs, (**8**) and (**9**), are only slightly favored at high temperature (e.g. at 328 K, which is near the T_m of most hybrids), whereas at room temperature they show a much higher affinity for DNA than the achiral PNA, with a stabilizing effect of 27.5 and 34.2 kJ/mol for the L-(**8**) and the D-enantiomer (**9**) respectively. Thus, the presence of lysine monomers in PNA oligomers induces a high DNA affinity at low ionic strength at room temperature. This may be exploited in diagnostic and molecular biology tool applications. However, the effect is absent at higher ionic strength (140 mM KCl), and thus should not enhance the antisense potency of these derivatives from an affinity point of view.

CD Spectroscopy

The CD spectra of the single strand PNAs and the antiparallel PNA-PNA duplexes were recorded in order to obtain information about the helix characteristics.

Neither the single stranded $T_{L\text{-}Leu}$-PNAs nor the $T_{L\text{-}Leu}$-PNA-PNA duplexes showed significant CD signals, indicating that the chiral centers failed to give a defined preferred handedness (data not shown).

In contrast, the T_{Lys}(middle)-PNAs, (**6**) and (**7**), showed strong signals of opposite signs for the PNA-PNA duplexes and similar but weaker signals for the single strands (Figure 4). In the case of the PNAs containing three lysine monomers in the strand, (**8**) and (**9**), the shape and the intensity of the spectra of the PNA-PNA duplexes were very similar to the T_{Lys}(middle)-PNAs, indicating that the handedness was mainly conferred by the central monomer. However, the CD spectra of the single strands were less well defined (Figure 5).

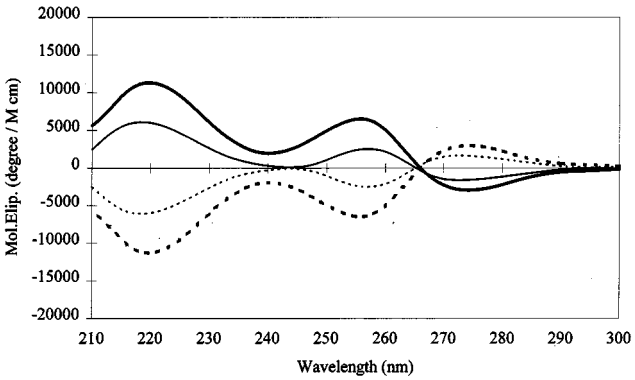

Figure 4. CD spectra of single strand T_{Lys}-PNAs and antiparallel T_{Lys}-PNA-achiral PNA duplexes. Thin broken curve: single strand $T_{L\text{-}Lys}$-PNA (**6**); thin solid curve: single strand $T_{D\text{-}Lys}$-PNA (**7**); thick broken curve: $T_{L\text{-}Lys}$-PNA (**6**) - achiral PNA duplex; thick solid curve: $T_{D\text{-}Lys}$-PNA (**7**) - achiral PNA duplex.

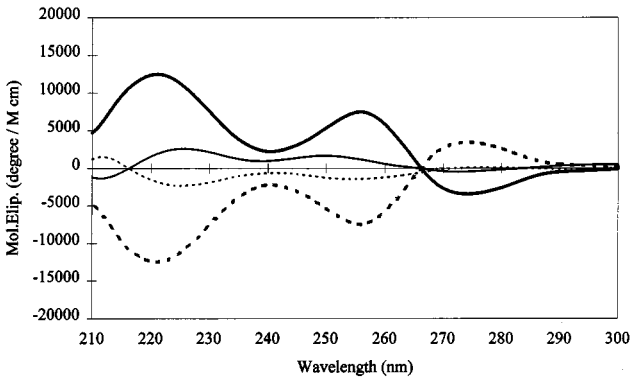

Figure 5. CD spectra of single strand $3T_{Lys}$-PNAs and antiparallel $3T_{Lys}$-PNA-achiral PNA duplexes. Thin broken curve: single strand $3T_{L\text{-}Lys}$-PNA (**8**); thin solid curve: single strand $3T_{D\text{-}Lys}$-PNA (**9**); thick broken curve: $3T_{L\text{-}Lys}$-PNA (**8**) - achiral PNA duplex; thick solid curve: $3T_{D\text{-}Lys}$-PNA (**9**) - achiral PNA duplex.

The PNAs bearing a lysine monomer at the C-terminus, (**4**) and (**5**), showed no CD signals in the single strands and a weak signal in the PNA-PNA duplexes (data not shown). As expected, in this case the sign of the CD bands in the absorbance region of the nucleobases was opposite (although the signals were weak), when comparing the D- and L-T_{Lys}-PNAs. Specifically, $T_{D\text{-}Lys}$(C-ter.)-PNA-PNA had a molar ellipticity of about −500 and $T_{L\text{-}Lys}$(C-ter.)-PNA-PNA of about +500 degree/M cm.

In order to further elucidate the effect of the amino acid side-chain in inducing a helical preference, PNAs containing monomers based on negatively charged amino acids (D-glutamic acid and L-aspartic acid) were also studied by CD spectroscopy. Although D-Glu and L-Asp are not enantiomers, differing by a methylene group in the side chain,

they can reasonably be taken as sufficiently close optical isomers. The same sequence was utilized and the three chiral monomers were inserted at the same positions: H-G*T*A-GA*T*CAC*T*-NH_2.

The $3T_{L\text{-}Asp}$- (**10**) and the $3T_{D\text{-}Glu}$-PNAs (**11**) were hybridized to the complementary antiparallel achiral PNA. The CD spectra of the duplexes and the single strands are reported in Figure 6.

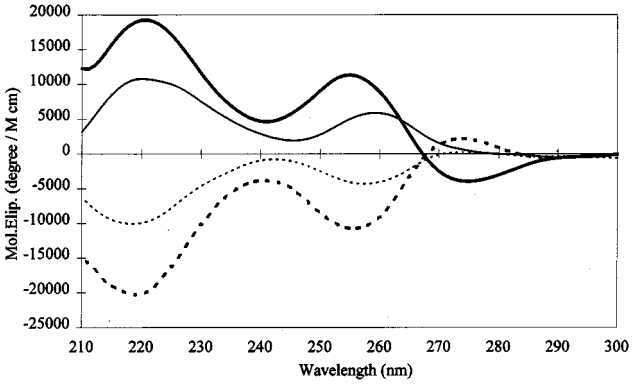

Figure 6. CD spectra of single strand $3T_{L\text{-}Asp}$- and $3T_{D\text{-}Glu}$-PNAs and antiparallel $3T_{L\text{-}Asp}$- or $3T_{D\text{-}Glu}$-PNA-achiral PNA duplexes. Thin broken curve: single strand $3T_{L\text{-}Asp}$-PNA (**10**); thin solid curve: single strand $3T_{D\text{-}Glu}$-PNA (**11**); thick broken curve: $3T_{L\text{-}Asp}$-PNA (**10**) - achiral PNA duplex; thick solid curve: $3T_{D\text{-}Glu}$-PNA (**11**) - achiral PNA duplex.

As already observed for T_{Lys}-PNAs, the CD spectra of the PNA-PNA duplexes showed a higher ellipticity, but were otherwise quite similar to the spectra of the single strand. This may indicates that a preferred handedness was already induced by the chiral centers in the single strand, and that this preference was enhanced in the duplex.

Furthermore, the helical preference of the $3T_{D\text{-}Glu}$-PNA (**11**) was identical to that observed for the $3T_{D\text{-}Lys}$-PNA (**9**), and the helical preference of the $3T_{L\text{-}Asp}$-PNA (**10**) was identical to that of the $3T_{L\text{-}Lys}$-PNA (**8**). Since the T_{Leu}-PNAs did not show significant CD signals, it is unlikely that the helical preference is due solely to steric factors. Indeed, the crystal structure of a PNA-PNA duplex[9] indicate absolutely no steric interference by either of the α-substituents. However, for the right-handed helix, the "L-substituent" is positioned to interact with the major groove, while the "D-substituent" is "pointing directly into solution". For the left-handed helix the situation is naturally reversed. Thus, the chemical functionality on the amino acid side chain is important. However, since two groups with opposite charges showed the same helical induction, we can deduce that the interaction involved is not a specific ion-dipole interaction or hydrogen bonding, but rather a solvation effect of the polar groups, which are likely to be shifted away from the PNA backbone because of water solvation. The induced conformational changes are transmitted to the closest base, thus modifying the stacking interactions and affecting the helical preference. In the single strand the same helical preference is present, although less pronounced because of the much weaker stacking interactions.

In order to better understand the influence of the chiral monomers on the structural organization of PNAs, we considered in more detail the PNA-PNA duplexes, which showed the higher ellipticity. By correlating the molar ellipticity of the PNA-PNA duplexes at 256 nm, interpreted as a significant parameter to assess the preference for one handedness, with the T_m of PNA-DNA duplex, i.e., to the stability of the hybrid, we observe that the higher the CD signal, the higher is the difference of melting temperatures between the duplexes formed by enantiomeric PNAs and the complementary DNA (Table 4). It is also noteworthy that, of a couple of enantiomers, the one giving higher T_m against DNA is always inducing a positive band in the spectrum of the PNA-PNA duplex at 256 nm.

The CD spectra of the T_{Lys}-PNA-DNA duplexes (both the L- and D- enantiomers), as well as those of the $T_{L\text{-}Leu}$-PNA-DNA duplexes (data not shown), closely resembled the CD spectrum of an achiral PNA-DNA duplex, although a decreased ellipticity in the 260 nm wavelength region is observed in all cases (Figure 7).

On the other side, the CD spectra of a DNA-DNA duplex and those of the separated strands are very similar (Figure 8), indicating that the DNA structure does not undergo dramatic changes upon duplex formation, probably due to its intrinsic rigidity.

Furthermore, the CD curves of both D- and L-Lys-PNA-DNA duplexes, as well as that of the achiral PNA-DNA duplex, are quite similar, suggesting that the preferred handedness of the duplex is dictated by the DNA. By subtracting the signal of the DNA strand from the CD spec-

Table 4. Correlation between the molar elipticity at 256 nm of the PNA-PNA duplexes and the difference of melting temperatures (ΔT_m) in the PNA-DNA duplexes for enantiomeric PNAs

	PNA-PNA		PNA-DNA		
Strand	$[\Theta]_D^{256}$	$[\Theta]_L^{256}$	T_{mD} (°C)	T_{mL} (°C)	$T_{mD} - T_{mL}$
T_{Lys} (C-term.) (**4**, **5**)	(−500)	(+500)	51	52	**−1**
Lys (C-term.)[a]	+5500	−5500	54[a]	51[a]	**+3**
T_{Lys} (middle) (**6**, **7**)	+6500	−6500	51	47	**+4**
$3T_{Lys}$ (**8**, **9**)	+7500	−7500	53	49	**+4**
$3T_{L\text{-}Asp}$ (**10**)	−	−10800	−	36[b]	**(+6)**
$3T_{D\text{-}Glu}$ (**11**)	+11200	−	42[b]	−	**(+6)**

[a] From ref.[2] — [b] From ref.[6]

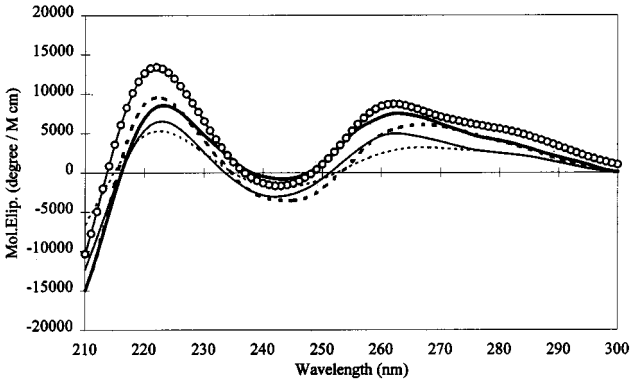

Figure 7. CD spectra of complementary antiparallel PNA-DNA duplexes. PNA sequences: Open circles: H-GTAGATCACT-NH_2; thin broken curve: $T_{L\text{-}Lys}$-PNA (**6**); thick broken curve: $3T_{L\text{-}Lys}$-PNA (**8**); thin solid curve: $T_{D\text{-}Lys}$-PNA (**7**); thick solid curve: $3T_{D\text{-}Lys}$-PNA (**9**).

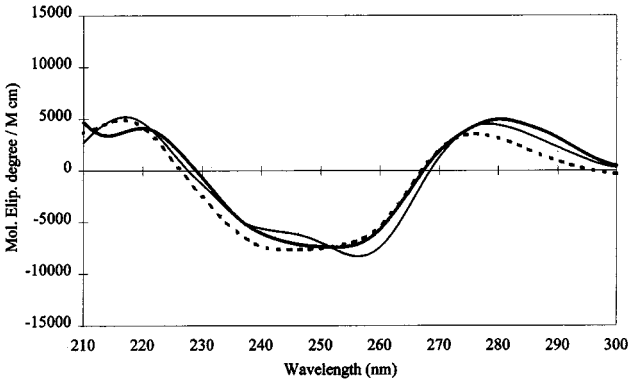

Figure 8. CD spectrum of a DNA-DNA antiparallel duplex compared with the spectra of the separated strands. Thick broken curve: DNA(1), 5′-dGTAGATCACT-3; thin broken curve: DNA(2), 5′-dAGTGATCTAC-3′; thick solid curve: DNA(1)-DNA(2) duplex.

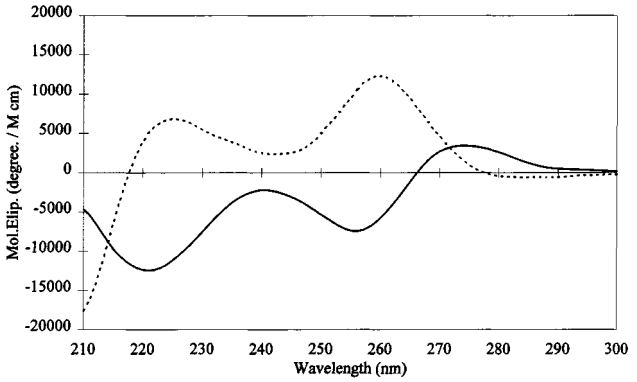

Figure 9. CD spectrum obtained by subtracting the DNA signal from the spectrum of $T_{L\text{-}Lys}$(middle)-PNA (**6**) − DNA antiparallel duplex (broken curve) compared to the CD spectrum of $T_{L\text{-}Lys}$-(middle)-PNA (**6**) − achiral PNA antiparallel duplex (solid curve).

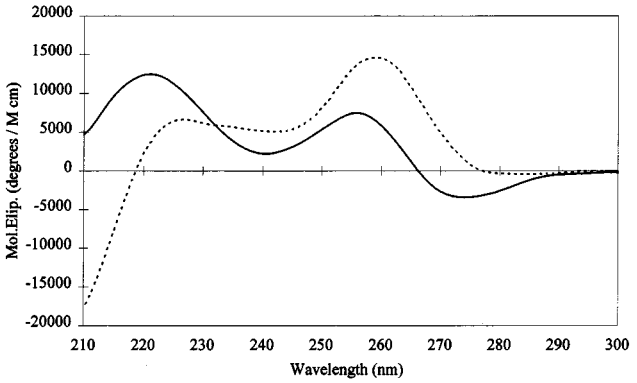

Figure 10. CD spectrum obtained by subtracting the DNA signal from the spectrum of $T_{D\text{-}Lys}$(middle)-PNA (**7**) − DNA antiparallel duplex (broken curve) compared to the CD spectrum of $T_{D\text{-}Lys}$-(middle)-PNA (**7**) − achiral PNA antiparallel duplex (solid curve).

trum of the PNA-DNA duplex, it is possible to obtain a CD spectrum essentially attributable to the PNA strand in the PNA-DNA duplex itself. In Figures 9 and 10 the CD spectra of the PNA-DNA duplexes after subtraction of the signal due to the DNA strand are shown and compared to the enantiomeric L-PNA-achiral PNA and D-PNA-achiral PNA duplexes. We conclude that both L- and D-PNA have a very similar conformation when complexed to DNA; and because the DNA itself is right-handed, both L- and D-PNA must have a right-handed helicity (when complexed to DNA). Additionally, if we compare the curves resulting after the subtraction of the DNA curve with those of the PNA-PNA duplexes, we must conclude that the $T_{D\text{-}Lys}$-PNA-PNA duplexes are right-handed, whereas the $T_{L\text{-}Lys}$-PNA-PNA duplexes are left-handed. The difference in stability observed for enantiomeric PNAs, when complexed to complementary DNA, is therefore attributable to the different preference for the right-handed helix, in which both PNAs are forced upon complexation.

This assignment is opposite to that proposed for PNA-PNA duplexes containing D- and L-lysine as terminal amino acid,[5] which was based on theoretical considerations and on similarities of CD spectra of DNA-DNA and PNA-PNA duplexes at longer wavelength. In fact, the DNA-DNA duplex has a positive band with a maximum at 275 nm and molar ellipticity of about +6500; the L-Lys-PNA-PNA has a positive band with a maximum at 270 nm and molar ellipticity of about +2000; the D-Lys-PNA-PNA has a negative band with a minimum at 270 nm molar ellipticity of about −2000. On these grounds, a right-handed helical conformation had been assigned to the L-Lys-PNA-PNA duplex. However, it is now known from crystallographic data[9] that the P-form of the PNA-PNA helix is very different from the classic B-form of DNA, so that any assignment of handedness, based either on CD similarities of different oligomers or theoretical calculations[11] assuming a B-like helix for PNA, is not straightforward.

Conclusions

Chiral charged monomers introduced in a PNA strand induce a preferred handedness in the PNA-PNA duplexes. The extent of the induced chirality depends upon the num-

ber of the monomers and their position in the strand. In particular, monomers containing amino acids with either a positively or a negatively charged side chain inserted in the middle of the strand exert the largest effect, indicating that solvation effects are mainly responsible for the preferred conformation. The sign of the charge on the amino acid side chain does not affect the preferred handedness, which essentially depends on the original configuration at the amino acid stereogenic center. The helix propagation most probably occurs through base stacking, since the preference becomes more pronounced in the duplex than in the single strand. According to the present results, the L-PNA-achiral PNA duplexes are left-handed, whereas the D-PNA-achiral PNA duplexes are right-handed.

As expected, the DNA-PNA duplexes are always right-handed, both with the L- and D-monomer containing PNAs. The relatively rigid structure of DNA forces both L- and D-PNAs to bind in a right-handed helicity. The D-PNA, which has a preference for right-handedness, is therefore favored in the binding, whereas the L-PNA must assume the unpreferred handedness. Thus, the complexation of DNA with chiral PNAs containing a charged side chain (Lys, Glu, Asp) is enantioselective. The difference in melting temperatures between PNA-DNA duplexes formed by enantiomeric PNAs clearly indicates that enantioselectivity is based on structural features. Thus, the preferred helical conformation induced by the stereogenic center in PNAs plays a definite role in DNA recognition. In the case of Lys-PNAs, a certain direction control is observed, in connection with the configuration of the stereogenic center.

The presence of charged chiral monomers only slightly preorganizes the single stranded PNAs, but it enhances significantly the helical preference of the PNA-PNA duplexes, as shown by circular dicroism.

Finally, the $3T_{Lys}$-PNAs, (**8**) and (**9**), show a very high affinity for DNA at low ionic strength, which is ascribed mainly to stabilizing electrostatic interactions. Therefore, the introduction of D-lysine monomers in PNAs should be an efficient way of enhancing the performance of PNA probes in diagnostic and molecular biology applications.

Experimental Section

General: DMF: *N*,*N*-dimethylformamide; HBTU: *O*-(1*H*-benzotriazol-1-yl)-*N*,*N*,*N*′,*N*′-tetramethyluronium hexafluorophosphate; TFMSA: trifluoromethanesulfonic acid; TFA: trifluoroacetic acid; EDTA: ethylenediaminotetracetic acid; Leu: leucine; Lys: lysine; Glu: glutamic acid; Asp: aspartic acid.

The abbreviations used for the nucleobases (T, C, A, G) indicate different chemical structures in PNA and DNA oligomers: in the former case the nucleobase is connected to a pseudopeptide backbone, in the latter to a sugar-phosphate one.

PNA chiral monomers incorporating thymine are indicated as T_{aa}, where aa is the abbreviation for the incorporated amino acid (i.e. the chiral monomer incorporating thymine and based on L-Lys is indicated as $T_{L\text{-}Lys}$); PNA oligomers bearing chiral monomers are indicated as T_{aa}-PNA, where T_{aa} indicates the number and the type of the chiral monomers inserted in the strand [i.e. $T_{L\text{-}Lys}$ (middle)-PNA is a decamer bearing one chiral T-monomer based on L-Lys in the middle of the strand, whereas $3T_{D\text{-}Lys}$-PNA has 3 chiral T-monomers based on D-Lys]. The sequences are given from the *N* to the *C* direction.

The achiral PNA monomers Boc-T_{Gly}-OH, Boc-$C(Z)_{Gly}$-OH, Boc-$A(Z)_{Gly}$-OH, and Boc-$G(Z)_{Gly}$-OH were commercially available from Perseptive Biosystems (Framingham, MA, USA). The Boc-T_{Leu}-OH, Boc-T_{Lys}-OH, Boc-T_{Glu}-OH, Boc-T_{Asp}-OH monomers were prepared as described in literature.[12] The oligomerization of PNAs was performed by means of the standard procedure on a (4-methylbenzhydryl)amine resin (Novabiochem) with HBTU/diethylcyclohexylamine as coupling reagent in DMF/pyridine.[12,13,15] The syntheses were performed on a 6 μmol scale. The free PNAs were cleaved from the resin using a TFMSA/TFA mixture (typical yields of the crude products: 70−90%). The crude PNAs were purified by HPLC (RP-C_{18} column, eluent: water-acetonitrile mixtures with 0.1% TFA, gradient: from 100% water to 100% acetonitrile in 25 minutes, flow 1 mL/min) and characterized by MALDI-TOF mass spectrometry on a Kratos Compact instrument using sinapinic acid as matrix (Table 5).

Table 5. MALDI-TOF mass spectra of T_{Leu} and T_{Lys}-PNAs

PNA	Calculated mw	Measured mw
$T_{L\text{-}Leu}$ (C-term.) (**1**)	2782.8	2782.9
$T_{L\text{-}Leu}$ (middle) (**2**)	2782.8	2783.0
$3T_{L\text{-}Leu}$ (**3**)	2895.0	2891.6
$T_{L\text{-}Lys}$ (C-term.) (**4**)	2797.8	2796.5
$T_{D\text{-}Lys}$ (C-term.) (**5**)	2797.8	2799.9
$T_{L\text{-}Lys}$ (middle) (**6**)	2797.8	2794.9
$T_{D\text{-}Lys}$ (middle) (**7**)	2797.8	2796.3
$3T_{L\text{-}Lys}$ (**8**)	2940.0	2938.3
$3T_{D\text{-}Lys}$ (**9**)	2940.0	2938.3

The enantiomeric purity of the chiral monomers and oligomers was checked by GC[14] (Chirasil-Val column) and was always found to be between 94 and 98%.

The decameric DNAs used in the hybridization experiments were courteously synthesized by Prof. Otto Dahl (Department of Organic Chemistry, The H. C. Ørsted Institute, Copenhagen, Denmark) by an automatic synthesizer.

All hybrid samples reported were incubated at 90°C for 5 minutes, then slowly cooled at room temperature. Samples not incubated as above described showed no different behaviors during T_m measurements. The melting temperatures were measured by UV spectroscopy on a Gilford response spectrophotometer in a 10 mM sodium phosphate buffer containing 100 mM NaCl and 0.1 mM EDTA, pH 7.0 (standard deviations were estimated as ±1°C). The melting temperatures used to determine thermodynamic parameters were measured in the same buffer without NaCl. The total strand concentration for each sample was calculated from the absorbance at 70°C using the following ε_{260} ($mM^{-1}\,cm^{-1}$) for the four bases: T 8.8, C 7.3, A 10.4, G 11.7.

Circular dicroism spectra were obtained on the same samples used for the T_m determination by employing a Jasco model J710 spectropolarimeter. The concentrations used for calculating the molar ellipticity were derived from the absorbances at 70°C recorded during the T_m measurements. The given molar ellipticity was calculated for the average base, assuming an average ε_{260} of 9.6 $mM^{-1}\,cm^{-1}$ per base. All spectra were zeroed, smoothed and treated with a noise reduction software.

Acknowledgments

We gratefully acknowledge Annette Jørgensen and Jolanta Ludwigsen for their technical assistance. This work has been partially supported by CNR(Consiglio Nazionale delle Ricerche-Progetto Finalizzato Biotecnologie), MURST (Ministero dell'Università e della Ricerca Scientifica e Tecnologica) and by the Danish National Research Foundation (Denmark).

[1] P. E. Nielsen, M. Egholm, R. H. Berg, O. Buchardt, *Science* **1991**, *254*, 1497−1500.
[2] M. Egholm, O. Buchardt, P. E. Nielsen, R. H. Berg, *J. Am. Chem. Soc.* **1992**, *114*, 1895−1897.
[3] M. Eriksson, P. E. Nielsen, *Quart. Rev. Biophysics* **1996**, *29*, 369−394.
[4] M. Egholm, O. Buchardt, L. Christensen, C. Behrens, S. M. Freier, D. Driver, R. H. Berg, S. K. Kim, B. Norden, P. E. Nielsen, *Nature* **1993**, *365*, 566−568.
[5] P. Wittung, P. E. Nielsen, O. Buchardt, M. Egholm, B. Norden, *Nature* **1994**, *368*, 561−563.
[6] B. Hyrup, P. E. Nielsen, *Bioorg. Med. Chemistry* **1996**, *4*, 5−23.
[7] S. C. Brown, S. A. Thomson, J. M. Veal, D. G. Davis, *Science*, **1994**, *265*, 777−780.
[8] M. Eriksson, P. E. Nielsen, *Nature Structural Biology*, **1996**, *3*(5), 410−413.
[9] H. Rasmussen, J. S. Kastrup, J. N. Nielsen, J. M. Nielsen, P. E. Nielsen *Nature Structural Biology.* **1997**, *4*, 98.
[10] L. Betts, J. A. Josey, J. M. Veal, S. R. Jordan *Science* **1996,** *270*, 1838−1841.
[11] P. Wittung, M. Eriksson, R. Lyng, P. E. Nielsen, B. Norden, *J. Am. Chem. Soc.* **1995**, *117*, 10167−10173.
[12] G. Haaima, A. Lohse, O. Buchardt, P. E. Nielsen, *Angew. Chem. Int. Ed. Engl.* **1996**, *35*, 1939−1942.
[13] A. Puschl, S. Sforza, G. Haaima, O. Dahl, P. E. Nielsen, *Tetrahedron Lett.*, **1998**, *39*, 4707−4710.
[14] R. Corradini, G. Di Silvestro, S. Sforza, G. Palla, A. Dossena, R. Marchelli, in preparation.
[15] L. Christensen, R. Fitzpatrick, B. Gildea, K. H. Petersen, H. F. Hansen, T. Koch, M. Egholm, O. Buchardt, P. E. Nielsen, J. Coull, R. H. Berg, *J. Pept. Sci.* **1995**, *3*, 175−183.
[16] L. A. Marky, K. J. Breslauer, *Biopolymers* **1987**, *26*, 1601−1620.
[17] S. Tomac, M. Sarkar, T. Ratilainen, P. Wittung, P. E. Nielsen, B. Nordén, A. Gräslund, *J. Am. Chem. Soc.* **1996**, *118*, 5544−5552.

Received July 24, 1998
[O98344]